

Stochastic approach to DNA breathing dynamics

Suman Kumar Banik, Tobias Ambjörnsson and Ralf Metzler (*)

NORDITA, Nordic Institute for Theoretical Physics – Blegdamsvej 17, DK-2100 Copenhagen, Denmark

PACS.87.15.Aa { Theory and modelling; computer simulation.

PACS.82.37.-j { Single molecule kinetics.

PACS.87.14.Gg { DNA, RNA.

Abstract. { We propose a stochastic Gillespie scheme to describe the temporal fluctuations of local denaturation zones in double-stranded DNA as a single molecule time series. It is demonstrated that the model recovers the equilibrium properties. We also study measurable dynamical quantities such as the bubble size autocorrelation function. This efficient computational approach will be useful to analyse in detail recent single molecule experiments on clamped homopolymer breathing domains, to probe the parameter values of the underlying Poland-Scheraga model, as well as to design experimental conditions for similar setups.

Introduction. { Under a large range of salt conditions and temperatures, the double-helix is the thermodynamically stable conformation of DNA [1,2]. This stability is effected by the Watson-Crick H-bonding of base-pairs (bps), and the stronger base-stacking of neighbouring, planar aromatic bps, that by hydrophobic interactions stabilize the helical structure [3,4]. At the same time, double-stranded DNA (dsDNA) is distinguished by the ease with which locally themolecule can open up (and later rejoin), to produce flexible bubbles of single-stranded DNA (ssDNA), see Gurela [1,2]. The formation of DNA-bubbles, despite the rather large enthalpy necessary to break the base-stacking, is made possible by the entropy gain, due to which the free energy for breaking additional bps is of the order of $k_B T$, after overcoming a bubble initiation barrier $\sim 10^5 :: 10^3$ [5]. At room or physiological temperature, bubbles of 20 to 30 broken bps are created [2]. DNA-bubbles preferentially form in regions rich in the weaker AT bps [5], and they are related to physiological processes such as transcription initiation [6].

Traditionally measured in bulk by UV-absorption at elevated temperatures [7], it is now possible to probe the time series of the size fluctuations of a single DNA-bubble (DNA-breathing) by fluorescence correlation techniques in short, designed DNA-stretches [8]. These DNA-constructs contain a well-defined $(AT)_n$ breathing domain, that is labelled by a fluorophore-quencher pair. Such a model system allows for a precise quantitative analysis, from which the parameters of the underlying theoretical model (usually the Poland-Scheraga model) can be determined. This fluorescence technique is being developed further to measure longer bubble domains, also at higher temperatures. It is therefore of interest to provide a theoretical model to understand DNA-breathing in a homopolymer domain quantitatively. One

(*) E-mail: metz@nordita.dk

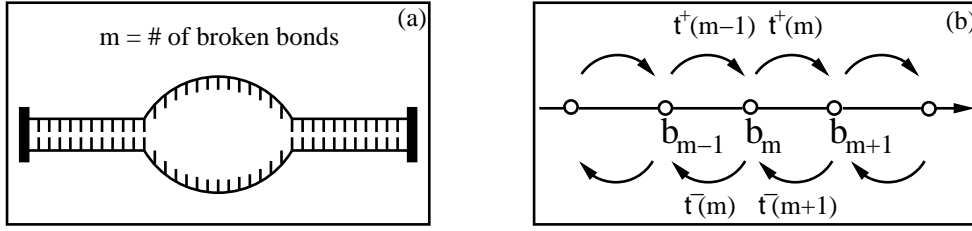


Fig. 1 { (a) A stretch of dsDNA that is clamped at both ends, with an ssDNA bubble consisting of m broken bps. (b) Schematic representation of the jump process underlying bubble-breathing.

possible approach is based on the master equation for the probability distribution to find a certain bubble size at time t , from which quantities such as the mean bubble size or the bubble autocorrelation function can be derived [9,11]. Despite its mathematically appealing formulation, the master equation needs to be solved numerically by inverting the transfer matrix [9,11]. Moreover, it produces ensemble-averaged information. Given the access to single molecule data, it is of relevance to obtain a model for the fully stochastic time evolution of a single DNA-bubble, providing a description for pre-noise-averaged quantities such as the step-wise (un)zipping. With this scope, we here introduce a stochastic simulation scheme for the (un)zipping dynamics. We use the Gillespie algorithm to update the state of the system by determining (i) the random time between individual (un)zipping events, and (ii) which reaction direction (zipping, $+$, or unzipping, $-$) will occur. We corroborate that the model recovers the equilibrium properties, and study the single bubble time evolution. The proposed scheme is efficient computationally, easy to implement, and amenable to generalization.

The Model. Motivated by the in vitro study of reference [8], we consider a dsDNA segment with M bps that is clamped at both ends (figure 1a). A bubble state of m broken bps is defined by the occupation numbers $b_m = 1$ and $b_{m \neq 0} = 0$ ($m \in \{0, \dots, M\}$). The stochastic simulation then corresponds to the nearest-neighbour jump process (figure 1b)

$$b_0 \quad b_1 \quad \dots \quad b_m \quad \dots \quad b_{M-1} \quad b_M ; \quad (1)$$

with reflecting boundary conditions at b_0 and b_M . Each jump away from state b_m occurs after a random time τ , and in random direction to either b_{m-1} or b_{m+1} , governed by the reaction probability density function (PDF) $P(\tau; \cdot)$ [12]

$$P(\tau; \cdot) = t(\cdot) e^{-t(\cdot)\tau} ; \quad (2)$$

where $t(\cdot)$ denotes the unzipping ($+$) or zipping ($-$) of a bp, and the jump rates $t(\cdot)$ are defined below. From the joint PDF \mathcal{P} , the waiting time PDF that a jump away from b_m occurs is given by $P(\tau; \cdot) = \mathcal{P}(\tau; \cdot)$, i.e., it is Poissonian. The probability that the bubble size does not change in the time interval $[0; \tau]$ is given by $\phi(\tau) = 1 - \int_0^\tau t(\cdot) \mathcal{P}(\tau - \tau'; \cdot) d\tau'$.

The rates $t(\cdot)$ are based on the statistical weight for a homopolymer bubble [2,13]

$$Z^m(m) = u^m (1 + m)^{-c} \quad (3)$$

according to the Poland-Scheraga model, with $Z^m(0) = 1$. Here, we introduced the loop initiation factor u for breaking the initially unperturbed dsDNA; the statistical weight

⁽¹⁾The original expression $P(\tau; \cdot) = b_m t(\cdot) \exp \left(-\sum_{m'} b_{m'} t(\cdot) \tau \right)$, that is relevant for consideration of multi-bubble states, simplifies here due to the particular choice of the b_m .

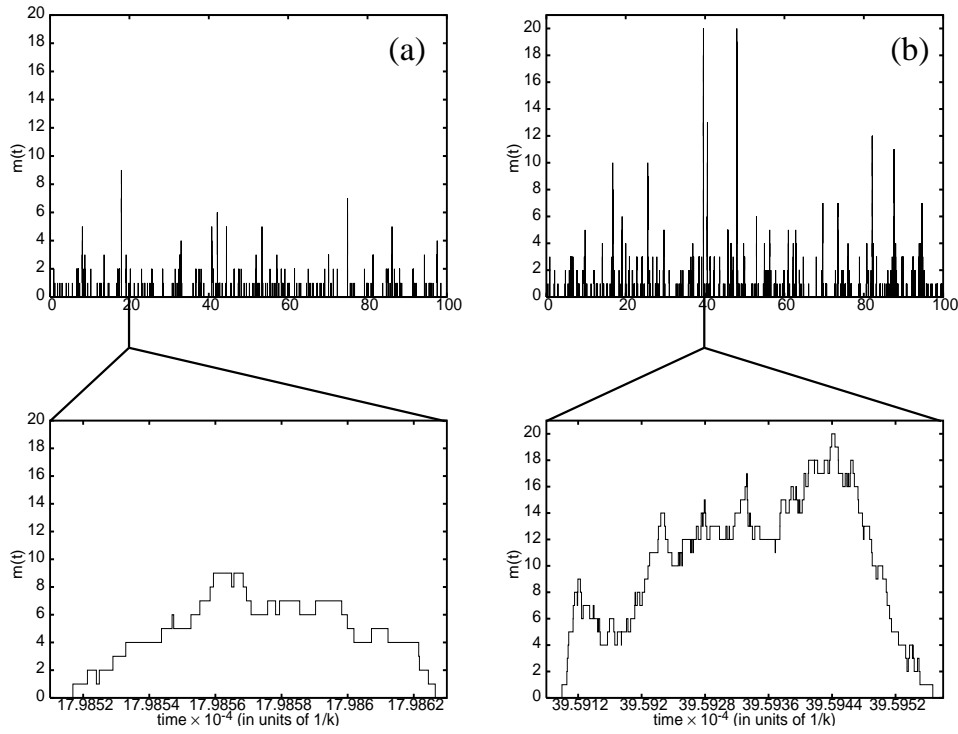


Fig. 2 { Time series of single bubble-breathing dynamics for $\phi_0 = 10^{-3}$, $M = 20$, and (a) $u = 0.6$ and (b) $u = 0.9$. The lower panel shows a zoom-in of how single bubbles of size $m(t)$ open up and close.

$u = \exp(-E/k_B T)$ with the free energy $E = E(T)$ associated with breaking an additional bp. For the (AT) domain (with melting temperature 67 C), $u = 0.6$ corresponds to physiological temperature, and $u = 0.9$ to 61 C. We note that in single molecule stretching experiments the effective temperature can be changed by applying an external torque T , such that $u \neq \exp(-\phi_0 T/k_B T)$, where $\phi_0 = 2\pi/10.35$ is the twist angle per bp of the dsDNA [14,15]. Equation (3) also introduces the loop closure factor $(1+m)^c$ assigned to the entropy loss for creating a polymer loop of size m ; the offset by 1 is due to persistence length corrections [5,16]. For the loop closure exponent in the rather short DNA-segment we have in mind here, we choose $c = 1.76$ [5,17,18], although higher values have been suggested [13]. Requiring that the system eventually reaches equilibrium, the rates $t^-(m)$ have to fulfil the detailed balance condition $t^+(m-1)Z^m(m-1) = t^-(m)Z^m(m)$. This condition does not fully specify the rates, and we choose the specific form [9,11]

$$t^+(0) = 2^c k_0 u; t^+(m) = k \frac{Z^m(m+1)}{Z^m(m)} = k u \frac{1+m}{2+m}^c; t^-(m) = k; \quad (4)$$

completed by $t^-(0) = t^+(M) = 0$. This choice assumes that the unzipping of a bp is limited by the Boltzmann factor u ($\phi_0 u$ for bubble initiation), whereas bp-zipping occurs with constant rate k , specified by the sterical formation of a bp (to be determined from microscopic models).

Results and discussions. { We start the simulations from the completely zipped state, $b_0 = 1$ at $t = 0$, and measure the bubble size at time t in terms of $m(t) = \sum_{m=0}^M m b_m(t)$. The

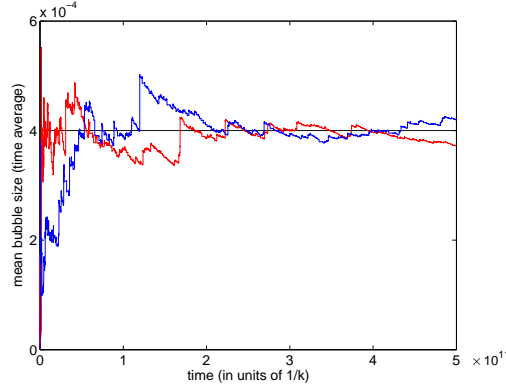


Fig. 3 { Running average of the bubble size $\overline{m}(t)$ for two realizations (rugged lines). The straight line represents the ensemble average $\lim_{t \rightarrow \infty} \overline{m}(t) = 4.05 \cdot 10^{-4}$ for $\rho_0 = 10^{-3}$, $u = 0.6$, and $M = 20$.

The time series of $m(t)$ for a single stochastic realization is shown in Figure 2. It is distinct that the bubble events are very sharp (note the time windows of the zoom-ins), and most of the time the zero-bubble state b_0 prevails due to $\rho_0 < 1$. Moreover, raising the temperature increases the bubble size and lifetime, as it should. By construction of the simulation procedure, it is guaranteed that an occupation number $b_m = 1$ ($m \neq 0$) corresponds to exactly one bubble.

To study the ergodicity of the stochastic simulation, we compare the running average

$$\overline{m}(t) = t^{-1} \sum_{i=0}^{N_t-1} m(t_i) : t_{i+1} - t_i = \tau_i; t_N - t_{N-1} = \tau_N; t_0 = 0 \quad (5)$$

of the bubble size with the ensemble average, $\lim_{t \rightarrow \infty} \overline{m}(t) = \langle m \rangle = \left(\rho_0 / N_1 \right) \sum_{m=1}^M m u^m (1+m)^c$, where $N_1 = 1 + \rho_0 \sum_{m=1}^M u^m (1+m)^c$. Note that in equation (5), we sample over the stochastic time steps t_i chosen from the reaction PDF (2), such that we need to weight the individual $m(t_i)$ by the time span τ_i until the next jump to $m(t_{i+1})$. For long times, the quantity (5) is expected to reach the equilibrium value given by the ensemble-average, i.e., $\lim_{t \rightarrow \infty} \overline{m}(t) = \langle m \rangle$. In Figure 3, we display the time evolution of $\overline{m}(t)$ for two different stochastic trajectories. Both approach the ensemble-average $\langle m \rangle$ for longer times. Relatively large deviations from $\langle m \rangle$ occur, corresponding to a lumping of small or large bubble states.

In Figure 4, we show the bubble size averaged exclusively over time steps τ_i during which $m(t_i) \neq 0$, as a function of the statistical weight u . As expected, the bubble size increases with increasing temperature, and the incorporation of the loop correction term distinctly reduces the maximum bubble size at equilibrium. The small error bars for the stochastic simulation data and the good agreement with the theoretical prediction $\sum_{m=1}^M m u^m (1+m)^c$ demonstrate the reliability of the Gillespie algorithm.

Figure 5 depicts the time-averaged bubble size distribution

$$\overline{P}(m; t) = t^{-1} \sum_{i=0}^{N_t-1} b_m(t_i) \tau_i; \quad (6)$$

for runs over a large number of jumps N (see below) to ensure that equilibrium is reached: $\lim_{t \rightarrow \infty} \overline{P}(m; t) = P_{eq}(m)$. $\overline{P}(m; t)$ is compared to the ensemble-averaged bubble distribution, $P_{eq}(m > 1) = \left(1 - \rho_0 \right) \sum_{m=1}^M u^m (1+m)^c$, with $N_2 = 1 + \rho_0 \sum_{m=1}^M u^m (1+m)^c$ and

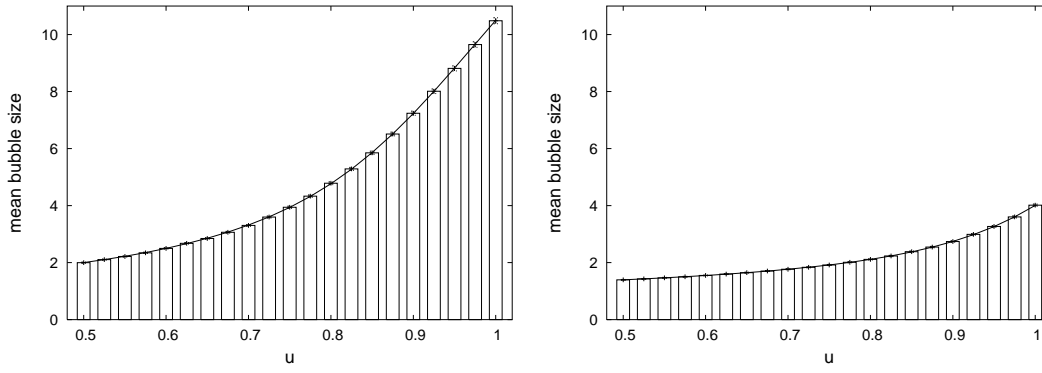


Fig. 4 { Mean bubble size m measured exclusively over open bubble states, as a function of statistical weight u with $c = 0$ (left) and $c = 1.76$ (right). The boxes represent the time average from the simulations, the full line is the ensemble-average. The parameters are $\rho_0 = 10^{-3}$ and $M = 20$.

$P_{eq}(0) = (1-N_2)$. This analysis demonstrates that the dsDNA segment almost always remains completely zipped (since $\rho_0 \ll 1$), note the logarithmic ordinate. At room temperature the formation of bigger bubbles is a rare event. Conversely, near the melting temperature bubble formation is significantly increased (see also figure 2b). Note that in figures 4 and 5, we chose the ordinates such that they span the same range for the simulated parameter values, to facilitate easy comparison. A gain, small error bars and good agreement of the time-average with the theoretical ensemble-average are distinct. The Gillespie algorithm governing our stochastic simulation therefore reliably leads to relaxation towards equilibrium, as it should, given that the detailed balance condition is fulfilled by the transfer rate coefficients $t(m)$.

We determine the time-averaged autocorrelation function through the discretized form

$$\overline{C}(t) = \frac{1}{N} \sum_{n=0}^{X^N} \frac{m(t+n_{bin})m(n_{bin})}{\overline{m}_1^2} \cdot \frac{1}{N} \sum_{n=0}^{X^N} \frac{m^2(n_{bin})}{\overline{m}_1^2} ; \quad (7)$$

Here, N is the number of sample points taken over the trajectory, with sampling time incre-

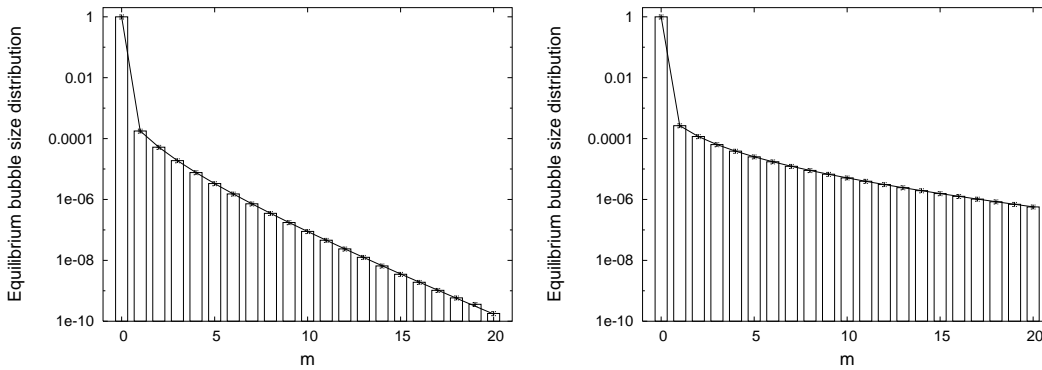


Fig. 5 { Equilibrium bubble size distribution for $u = 0.6$ (left) and $u = 0.9$ (right) ($\rho_0 = 10^{-3}$). The boxes represent the simulations result ($\overline{P}(m;t)$), the full line is the theoretical prediction ($P_{eq}(m)$).

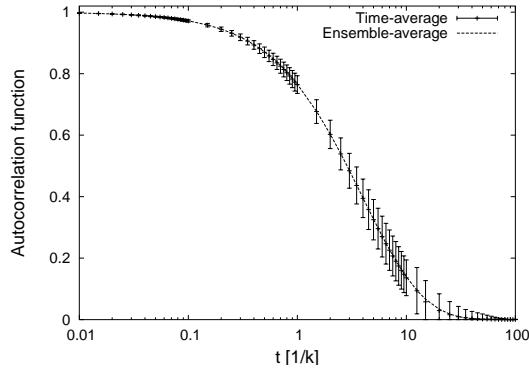


Fig. 6 { Time-averaged ($\bar{C}(t)$) and ensemble-averaged ($C_{eq}(t)$, see [9,11]) autocorrelation functions versus correlation time for $\phi_0 = 10^{-3}$, $u = 0.6$, $c = 1.76$, and $M = 20$.

ments $\phi_{bin} = \phi/k$. We chose 10^4 . Figure 6 displays the bubble size autocorrelation $\bar{C}(t)$ as obtained from the stochastic simulation in comparison to the ensemble-averaged correlation $C_{eq}(t) = \langle m(t)m(0) \rangle / \langle m^2 \rangle$; the latter is obtained by numerically solving the eigenvalue problem associated with the master equation, see references [9,11]). Both show good agreement. From $\bar{C}(t)$, we conclude that at $u = 0.6$, the typical bubble lifetime should be of the order of $20/k$. Given the typical experimental bubble lifetime $\tau \approx 1$ ms at room temperature, we extract that the zipping rate $k \approx 50$ sec, consistent with reference [8].

Implementation. { To determine the random waiting time and the random reaction channel in the jump process (1) controlled by the reaction PDF $P(\cdot; \cdot)$, two independent random numbers r_1 and r_2 ($r_1 \in [0;1]$) are generated. In the "direct method", one conditions the reaction PDF in the form $P(\cdot; \cdot) = \langle \cdot \rangle P_c(\cdot)$, where $P_c(\cdot)$ is the probability that the next reaction is a jump, given that the next reaction occurs at time $t + \Delta t$ [12]. The waiting time can then be obtained through the relation [12]

$$t = -\ln(1-r_1) = -\ln(t^+ + t) \ln(1-r_1): \quad (8)$$

From r_2 , the direction of the jump is determined as \pm , if $0 < r_2 [t^+ + t] - t$ holds; otherwise, $\pm = +$ [12]. A typical run would sample over 10^{10} to 10^{12} jumps to produce a single time series trajectory, where, in general, lower temperature requires longer runs. To ensure that equilibrium was reached in such a run, we checked that the quantity of interest reached (almost) constant values. For the correlation function, about 10^7 jumps were sampled at increments of $10^{-4}/k$. For the time-averages, we calculated the mean over 100 trajectories.

Conclusions. { By stochastic simulation based on the Gillespie algorithm, we obtained the time series of the breathing fluctuations of a single homopolymer DNA bubble, inspired by well-defined DNA-constructs employed in recent single molecule fluorescence correlation experiments. The waiting time for a jump event corresponding to a single zipping or unzipping event defined by the reaction PDF is Poissonian; however, due to the Boltzmann factors in the rates, the mean waiting time for a jump to occur can become quite long.

To corroborate that the stochastic simulation properly describes thermalization, we determined equilibrium properties such as the mean bubble size and its distribution from time-averaging, to find almost perfect agreement with the calculated ensemble-averaged values. We also showed that the bubble size autocorrelation function and the running average of the

bubble size follow the behaviour predicted by the master equation. The stochastic scheme is therefore a reliable way to describe the bubble dynamics. Computationally, the scheme is quite efficient, and it can be implemented in a straightforward manner.

The major advantage of the stochastic approach, similar to the Langevin picture in diffusion processes, is the possibility to sample single stochastic trajectories and thereby study the direct effect of changes in the physical parameters (initiation factor ρ_0 , statistical weight u , loop closure factor c) on the single bubble time series. This is particularly relevant as it is possible, with the current experimental means, to record single bubble time series. Given the good convergence of the statistical sampling, comparison of dynamical data as obtained from our algorithm to experimental or precise microscopic simulations data will be an important way to explore further the validity of the Poland-Scheraga approach to DNA-breathing, in particular, the exact value of the loop closure exponent c and the bubble initiation factor ρ_0 , as well as potential corrections in the Poland-Scheraga model for small bubble domains.

Further advantages are the relatively straightforward possibility to include types of waiting times that are different from the Poissonian, for instance long-tailed ones [19]. The stochastic simulation is also more flexible to easily incorporate additional features such as the coupling to the binding dynamics of selectively single-stranded binding proteins to the fluctuating bubbles, sequence heterogeneity, or multiple bubbles, due to the formulation of an arbitrary number of coupled reactions in the Gillespie algorithm. The corresponding master equation approach in such cases quickly becomes intractable, once the number of variables exceeds two. It may therefore be desirable to have available a stochastic simulation package designed for DNA-breathing similar to the program MELT SIM for DNA melting simulations [5].

We acknowledge very helpful discussions with Andreas Isacson, and thank Petter Urdedal for assistance with the Intel Fortran compiler.

REFERENCES

- [1] Kornberg, A., DNA Synthesis (W. H. Freeman, San Francisco, CA) 1974.
- [2] Poland, D. and Scheraga, H. A., Theory of helix-coil transitions in biopolymers (Academic Press, New York) 1970.
- [3] Watson, J. D. and Crick, F. H. C., Cold Spring Harbor Symp. Quant. Biol., 18 (1953) 123.
- [4] Delcourt, S. G. and Blake, R. D., J. Biol. Chem., 266 (1991) 15160.
- [5] Blake, R. D. et al., Bioinformatics, 15 (1999) 370.
- [6] Kornberg, A. and Baker, T. A., DNA Replication (W. H. Freeman, New York, NY) 1992.
- [7] Wartell, R. M. and Benight, A. S., Phys. Rep., 126 (1985) 67.
- [8] Altan-Bonnet, G., Libchaber, A. and Krichevsky, O., Phys. Rev. Lett., 90 (2003) 138101.
- [9] Ambjornsson, T. and Metzler, R., E-print, (q-bio.BM/0411053).
- [10] Hanke, A. and Metzler, R., J. Phys. A, 36 (2003) L473.
- [11] Ambjornsson, T. and Metzler, R., J. Phys. Cond. Mat., 17 (2005) S1841.
- [12] Gillespie, D. T., J. Comp. Phys., 22 (1976) 403; J. Phys. Chem., 81 (1977) 2340.
- [13] Richard, C. and Guttmann, A. J., J. Stat. Phys., 115 (2004) 925.
- [14] Cocco, S., Monasson, R. and Marko, J. F., Proc. Natl Acad. Sci., 98 (2001) 8608.
- [15] Pant, K., Karpel, R. L. and Williams, M. C., J. Mol. Biol., 327 (2003) 571.
- [16] Fixman, M. and Freire, J. J., Biopolymers, 16 (1977) 2693.
- [17] Fisher, M. E., J. Chem. Phys., 38 (1966) 112.
- [18] Hanke, A. and Metzler, R., Phys. Rev. Lett., 90 (2003) 159801.
- [19] Metzler, R. and Klafter, J., J. Phys. A, 37 (2004) R161.